Article

Transactions of the Institute of Measurement and Control
1–13

DOI: 10.1177/0142331215606514
tim.sagepub.com
SAGE

An intelligent algorithm for maximum power point tracking in photovoltaic system under partial shading conditions

Qichang Duan[1], Mingxuan Mao[1], Pan Duan[2] and Bei Hu[1,3]

Abstract

In a photovoltaic (PV) system, maximum power point tracking (MPPT) under partial shading (PS) conditions is a challenging task due to the presence of multiple peaks in the power voltage characteristics. This paper puts forward a novel artificial fish-swarm algorithm (FSA), which is optimized by particle swarm optimization with extended memory (PSOEM-FSA). In this algorithm, both the velocity inertia factor and the memory and learning capacity of PSOEM are introduced into the FSA. To validate the effectiveness of the novel algorithm, the PV system along with the proposed MPPT algorithm was simulated using Matlab/Simulink Simscape tool box. The simulation results show that the proposed approach is effective in MPPT under PS conditions and has a more stable performance when compared with the traditional methods in convergence speed and searching precision.

Keywords

Artificial fish-swarm algorithm (FSA), behaviour pattern, maximum power point tracking (MPPT), particle swarm optimization with extended memory (PSOEM), photovoltaic system

Introduction

Solar energy is widely used due to its noiseless and non-pollution characteristics, and many researchers have concentrated on developing photovoltaic (PV) generation. In addition, a PV system has many advantages including low maintenance and long life cycle.

Despite the high cost of solar modules, PV power generation systems, in particular the grid-connected type, have been commercialized in many countries because of their potential long-term benefits (Agorreta et al., 2011; Figueres et al., 2009; Liu et al., 2011; Serban and Serban, 2010; Yang et al., 2010; Young-Hyok et al., 2011; Zhang et al., 2011). However, maximum power extraction from the PV source is a challenging task because of its non-linear characteristics, which change with environmental conditions (Wang and Hsu, 2010). Some studies have shown that conventional maximum power point tracking (MPPT) operated on a sensing current. There exist some commercially well-known MPPTs, such as perturb and observe (P&O) (Femia et al., 2005, 2011), incremental conductance (INC) (Mei et al., 2011; Safari and Mekhilef, 2011) and hill climbing (HC) (Alajmi et al., 2011).

In addition, soft-computing techniques are catching the interest of researchers for their effectiveness, low cost, robustness and their global peak search capability. Various studies have exploited soft computing methods, which include particle swarm optimization (PSO), enhancing the solution of particles in the search space with a simplified mathematical function for the global maximum power point (MPP) (Ishaque et al., 2012). A fuzzy logic controller creates automatic control for non-linearity and unpredictable variations in the operating point that significantly deals with MPP (Nopporn et al., 2005; Syafaruddin et al., 2009). Messai et al. (2011) proposed that the genetic algorithm (GA) is an issue-resolving technique based on biological evolution and a population search that finds the best solution with a random gene combination. The voltage or duty cycle parameter in finding MPP has been exploited. Several of the soft computing MPPT techniques have proved to provide better capabilities than conventional techniques.

Based on the above analysis, a novel control algorithm called PSOEM-FSA is presented in this paper. The control method uses a simplified particle swarm optimization (PSO) algorithm to optimize the artificial fish-swarm algorithm (FSA). Such a novel control method is applied to predict the optimal output voltage values for a small practical PV panel. The control algorithm for the system to achieve maximum

[1]Automation College, Chongqing University, Chongqing 400044, China
[2]State Grid Chongqing Electric Power Company Nan'an Power Supply Subsidiary Company, Chongqing, China
[3]Chongqing University of Science and Technology, Chongqing 401331, China

Corresponding author:
Mingxuan Mao, Automation College, Chongqing University, Shapingba District, 174#, Chongqing City, Chongqing 400044, China.
Email: mx_m@cqu.edu.cn

power generation and the implementation procedure are explained. Finally, the PSOEM-FSA method is applied to control a PV system under PS conditions on the experimental platform. Experimental results are presented showing that the PV system tested generates higher output power using the new control method compared with using the conventional techniques and the PSOEM-FSA method outperforms the PSO-FSA method and the traditional point-by-point comparison method on the stability of the output power when the PV system is under various PS conditions.

The remainder of the paper is organized as follows: in the next section, the block diagram of an MPPT system is described. The proposed algorithm and the flowchart of PSOEM-FSA for MPPT are introduced, then the PV system model under PS conditions is presented. The high performance of PSOEM-FSA for MPPT under PS conditions is demonstrated and, finally, the conclusion and future work are proposed.

PV power generation system

In order to track the MPP in multiple PV solar cells, an understanding of how each PV cell works is mandatory. Each MPPT system is a combination of different PV cells connected in series or parallel, a DC–DC converter and the MPPT block (Femia et al., 2005). Figure 1 shows the structure of an MPPT system, which includes a PV panel emulator, solar MPPT DC–DC evaluation module (EVM; interleaved boost & HB resonant LLC), solar DC–AC inter EVM (full bridge DC–AC), isolated general-purpose input/output (GPIO) and communication interface (ribbon cable), and emulated grid consisting of resistive load, isolation transformer 1000 VA and AC source 1000 VA.

Figure 2 shows the DC–DC interleaved boost converter control loops. It uses current mode control. The goal is to control the PV panel output (Vpv), which is the input to the DC–DC stage. This allows the PV panel (array) to operate at its MPP at all times. Input current is regulated by adjusting the duty cycles of the power switches. Input voltage is regulated by adjusting the input current. An MPPT algorithm described in the next section is responsible for determining the set point (Vpv_ref) for the PV panel voltage. Notice that the input voltage control loop works quite differently compared with the conventional feedback used in output voltage control. Under this control scheme, when the PV panel voltage (Vpv) tends to go higher than the reference panel voltage (Vpv_ref) set by the MPPT algorithm, the control loop increases the panel current command (reference current for inner current loop Iind_ref) and thereby controls the panel voltage at its reference level (Vpv_ref). When the panel voltage tends to go lower than the reference, the control loop reduces the panel current command in order to re-establish the panel voltage to its reference level.

The proposed algorithm for MPPT

As stated above, the main objective of this paper is to assess the contribution of merging the extended memory and PSO algorithm into FSA for MPPT. The two key components of the proposed algorithm are PSOEM (Duan et al., 2011) and the improved fish behaviour patterns. In the following subsection, we will detail them and explain how they work together seamlessly.

The standard PSO

The standard PSO (Duan et al., 2011; Ishaque et al., 2012) is shown as follows:

$$v_{t+1} = \omega\, v_t + \alpha_t^l\left(p_t^l - x_t\right) + \alpha_t^g\left(p_t^g - x_t\right) \tag{1}$$

$$x_{t+1} = x_t + v_{t+1} \tag{2}$$

where subscript t denotes the index of iteration; v_t represents the speed of the particle in the tth iterative process; x_t represents the speed of the particle in the tth iterative process; p_t^l represents the current individual extreme value point of the particle in the tth iterative process; p_t^g represents the current global extreme value point of the population in the tth iterative process; ω is known as the inertia weight; c_1 and c_2 are

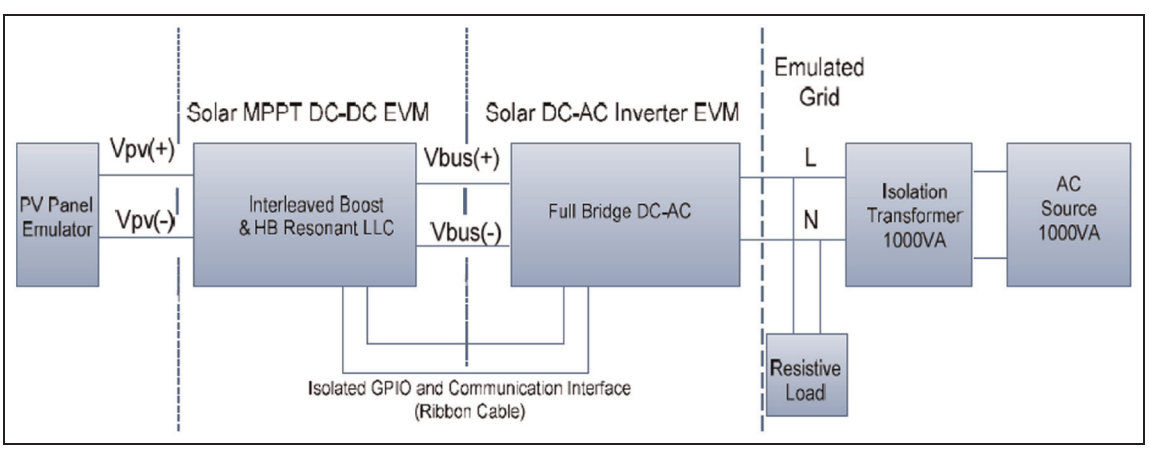

Figure 1. Diagram of an maximum power point tracking (MPPT) system.

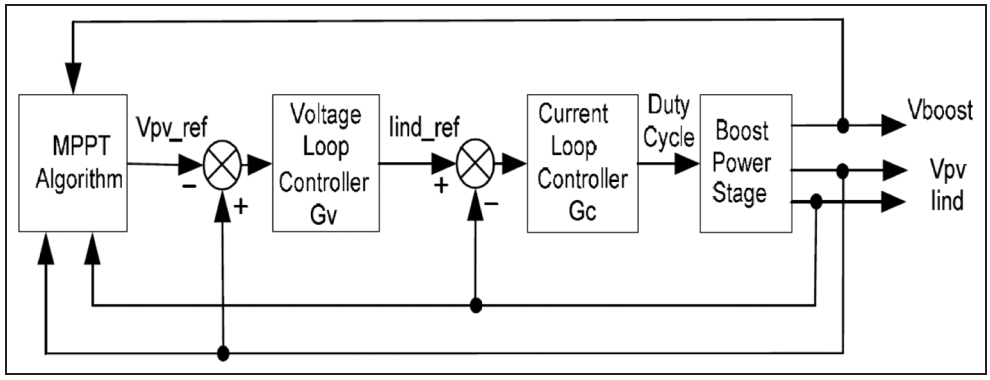

Figure 2. Maximum power point tracking (MPPT) DC–DC converter control loops.

treated as the acceleration factors, and $\alpha_t^l = c_1 r_1$, $\alpha_t^g = c_2 r_2$, r_1, $r_2 \sim U(0,1)$, ω, α_t^l, $\alpha_t^g \in R$, $\alpha_t^l \sim U(0,c_1)$, and $\alpha_t^g \sim U(0,c_2)$.

Improved PSO. PSO, a relatively new evolutionary computation model, has attracted extensive concern of researchers and experts in different areas in the past 10 years, and the various kinds of improved PSO have been presented. PSOEM combines several improved PSO algorithms, making full use of their advantages (Duan et al., 2011). From a psychological point of view, expanded memory means that the individual accumulates the search experience, which is conducive to improve the convergence speed. PSOEM can be expressed as follows:

$$\begin{aligned} v_{t+1} = \omega\, v_t &+ \alpha_t^l\left[\xi_t\left(p_t^l - x_t\right) + \xi_{t-1}\left(p_{t-1}^l - x_{t-1}\right)\right] \\ &+ \alpha_t^g\left[\xi_t\left(p_t^g - x_t\right) + \xi_{t-1}\left(p_{t-1}^g - x_{t-1}\right)\right] \end{aligned} \tag{3}$$

where $p_{t-1}{}^l$ represents current extreme value point of the particle in the $t-1$th iterative process; $p_{t-1}{}^g$ represents the current global extreme value point of the population in the $t-1$th iterative process; ξ_t is called current effective factor; ξ_{t-1} is called effective factor of extended memory, and $x_{t+1} = x_t + v_{t+1}$, $\xi_t, \xi_{t-1} \in R^+$, $\sum \xi_i = 1$. In particular, when $\xi_{t-1} = 0$, that is, $\xi_t = 1$, then (3) = (1). In this sense, PSO is a special case of PSOEM.

The proposed algorithm

Being attracted by the potential of FSA, many improved algorithms based on the ordinary FSA have been proposed, such as the introduction of the taboo optimization operator, fish jumping behaviour and fish memory behaviour, etc. In the proposed algorithm, the various characteristics of PSOEM, including speed inertia, the memory (learning) of individual particle, and information exchange and sharing between particles, respectively, are introduced into the FSA, and then PSOEM-FSA is put forward. The improvements of the proposed algorithm are expressed as follows.

At first, the speed parameter is introduced into each of the artificial fishes. Taking the swarm behaviour for example, the updated speed formula can be represented as follows:

$$V_{t+1} = \omega V_t + rand \times \frac{Step \times (X_t^c - X_t)}{\mathrm{norm}(X_t^c - X_t)} \tag{4}$$

where ω is the inertia weight; v_t represents the velocity vector of the artificial fish in the tth iterative process; Step is the largest mobile Step length; $X_t{}^c$ is the centre of the cluster behaviour vector; X_t represents the current position vector of the artificial fish in the tth iterative process; *norm* $(X_t{}^c - X_t)$ represents the distance between the two position vector, and $rand \sim U(0,1)$.

Secondly, the memory behaviour pattern is introduced. This behaviour makes the artificial fish swimming refer to its own optimal position, which can reduce the blindness of the fish in the search process. The updated speed is shown in Equation (5).

$$V_{t+1} = \omega V_t + rand \times \frac{Step \times \left[\xi_t(X_t^{pbest} - X_t) + \xi_{t-1}\left(X_{t-1}^{pbest} - X_{t-1}\right)\right]}{\mathrm{norm}\left[\xi_t(X_t^{pbest} - X_t) + \xi_{t-1}\left(X_{t-1}^{pbest} - X_{t-1}\right)\right]} \tag{5}$$

where X_t^{pbest} represents the optimal position vector of the artificial fish on the bulletin board in the tth iterative; $X_{t-1}{}^{pbest}$ represents the optimal position vector of the artificial fish on the bulletin board in the $t-1$th iterative process.

Thirdly, the communication behaviour pattern is introduced. This behaviour makes the artificial fish swimming refer to the optimal position of the whole fish, which strengthens the ability of exchanging and sharing information between the individual in the search process, and further reduces the blindness of the fish in the search process. The updated speed is shown in Equation (6).

$$V_{t+1} = \omega V_t + rand \times \frac{Step \times \left[\xi_t(X_t^{gbest} - X_t) + \xi_{t-1}\left(X_{t-1}^{gbest} - X_{t-1}\right)\right]}{\mathrm{norm}\left[\xi_t(X_t^{gbest} - X_t) + \xi_{t-1}\left(X_{t-1}^{gbest} - X_{t-1}\right)\right]} \tag{6}$$

where X_t^{gbest} represents the current global extreme value point of the population on the bulletin board in the tth iterative process; $X_{t-1}{}^{gbest}$ represents the current global extreme value

point of the population on the bulletin board in the $t-1$th iterative process.

Vision and step length are two very important parameters for FSA, and have an important effect on the optimization result. In this paper, we dynamically define the maximum distance as the vision and step length of the fish, which make two random fish may appear to be in the D dimension search space. Furthermore, we define the maximum distance as the MaxD, as shown in Equation (7).

$$MaxD = \sqrt{(x_{max} - x_{min})^2 \times D} \tag{7}$$

where x_{max} and x_{min} respectively represent the upper and lower bound of the optimization range; Visual is set to the linear gradient from MaxD to 0.01 MaxD; Step is set to the linear gradient from MaxD/5 to 0.

The specific process of PSOEM - FSA is shown as follows:

1) Initialize the position and speed of the fish, the optimal locations of each fish's memory and the optimal position parameters recorded on the bulletin board;
2) Test the four kinds of combination behaviour patterns: cluster or foraging, collision or foraging, memory or foraging, and communication or foraging;
3) Select the optimal combination behaviour model from (b) and use the speed update current location of the artificial fish;
4) If the specified number of iterations is available, the optimization will end, otherwise go to step (b).

Furthermore, the flowchart of the proposed algorithm is shown in Figure 3.

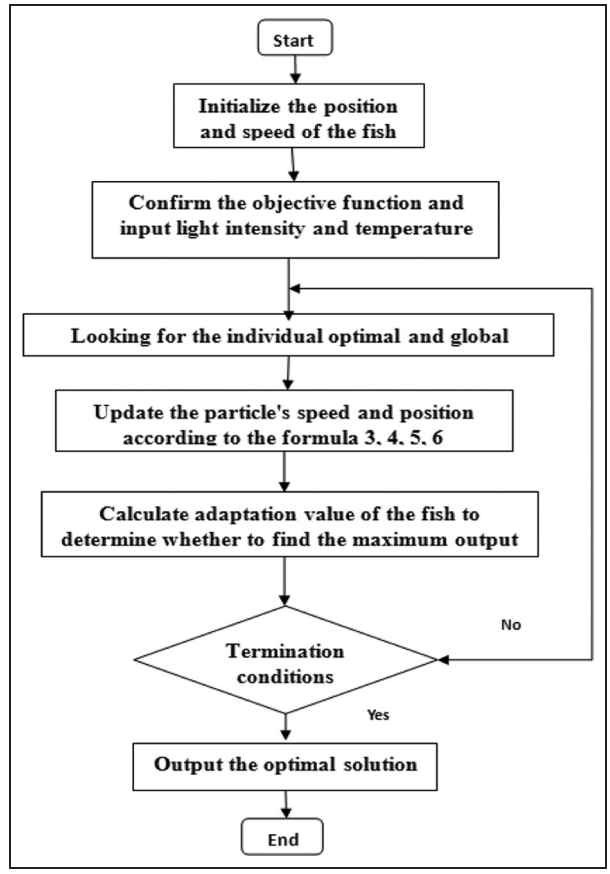

Figure 3. Flowchart of particle swarm optimization with extended memory of fish-swarm algorithm (PSOEM-FSA) for maximum power point tracking (MPPT).

PV system under PS conditions

At present, many researchers have concentrated on the development and utilization of renewable energy. PV power generation is one of the important branches. It is well known that PV power generation systems use PV arrays to absorb solar energy and convert it into electricity. A PV array is made up of many independent PV cells according to certain series–parallel rules.

Battery model

PV cells under PS conditions may obtain negative voltage. As the battery obtains a negative voltage, the current will increase dramatically when the reverse voltage on the PN junction increases towards a threshold, because the battery is similar to the PN junction diode, this phenomenon is called the avalanche breakdown effect. The model with a double diode with a reverse avalanche breakdown effect is shown in Figure 5, where V is the port voltage of PV battery, I_{ph} is the PV current, I_{D1} and I_{D2} are the currents through the diode $D1$ and $D2$, respectively, I is output current of the PV battery, I_V is the reverse avalanche breakdown current, and R_s and R_{sh} are the equivalent series resistance and shunt resistance, respectively.

According to Kirchhoff's first law:

$$I = I_{ph} - I_{D1} - I_{D2} - I_V - I_{sh} \tag{8}$$

$$I_{D1} = I_{s1}\left\{\exp\left[\frac{q(V + R_s I)}{A_1 KT}\right] - 1\right\} \tag{9}$$

$$I_{D2} = I_{s2}\left\{\exp\left[\frac{q(V + R_s I)}{A_2 KT}\right] - 1\right\} \tag{10}$$

$$I_{sh} = \frac{V + R_s I}{R_{sh}} \tag{11}$$

where I_{s1} and I_{s2} are the reverse saturation current of diode $D1$ and $D2$, respectively; A_1 and A_2 are the quality factors of diodes $D1$ and $D2$, respectively; q is the electron charge (1.609×10^{-19} C); T is the cell absolute temperature (K), and K is Boltzmann's constant (1.38×10^{-23} J/K).

PV array's mathematical model

When the PV array is in a uniform illumination, the output power of the array–voltage characteristic curve is in the shape of a single peak. Conversely, when some panels are under PS conditions, the characteristic curve will present a multiple

peak shape (Carannante et al., 2009; Lei et al., 2011; Patel and Agarwal, 2008). Furthermore, PS causes power losses through different mechanisms, the most severe one being the incoherence of the array's MPP with the modules' MPPs. This means that the MPP operation of the array does not coincide with the MPP operation of the individual modules; therefore, the overall operation is not optimal (Kadri et al., 2011). In addition to the previous mechanisms, PS increases the probability of the MPPT being misled to operate at local maxima, which will increase the losses (Mei et al., 2011).

Under PS conditions, the traditional MPPT methods, such as the P&O method, the INC method and so on, easily fall into local optima (Ishaque et al., 2012; Syafaruddin et al., 2009). Hence, a novel MPPT method, PSOEM-FSA, is put forward in this paper. This algorithm can easily avoid the limitation of local optimum, and find the global MPP under PS conditions.

Taking the branch current as the optimization variable, the fitness function is *P–I* relationship of the series branch (Duan et al., 2013), as shown in Equations (12) and (13).

$$fit = I \times \sum_{k=1}^{n_s} PVprog(i_k, Sun_k, T_k),\ n_s = 10 \tag{12}$$

$$PVprog(I, Sun, T) = 1.1103 \times log_{10}\left(\frac{3.8 \times Sun - I + 2.2 \times 10^{-8}}{2.2 \times 10^{-8}}\right) - 0.2844 \times I \tag{13}$$

where $PVprog(I, Sun, T)$ represents the output power of each of PV panels–current characteristic function; Sun and T represent the light intensity and environment temperature, respectively.

Experiments and discussion

To evaluate and analyse the performance of the proposed algorithm, we perform numerical simulation with Matlab7.1. Firstly, a number of numerical simulation experiments are done to compare the performance of PSOEM-FSA with the other algorithms, including the PSO algorithm (Banks et al., 2007), FSA (Li et al., 2002) and PSO-FSA (Duan et al., 2013), under the same parameter settings.

Numerical simulation analysis

Experimental settings. Experiments are performed on four benchmark functions that are often used as measurement criteria of optimization algorithms in continuous and static spaces. Benchmark functions with their optimum value and optimum range are presented in Table 1 (Zhan et al., 2009). It should be noted that optimal value of all these function equals zero. In addition, the sphere function is a single-peak function, and the others are multi-peak functions. They are used to investigate the effect of PSOEM-FSA, PSO algorithm, FSA and PSO-FSA.

To make a fair comparison between PSO (Banks et al., 2007), FSA (Li et al., 2002), PSO-FSA (Duan et al., 2013) and PSOEM-FSA, these algorithms adopt the parameter settings in Table 2. Furthermore, all algorithms run 50 times independently and are stopped when the maximum number of 1000 function evaluations (FES) is reached.

Table 1. Parameters of the algorithm.

	Parameter	Value
PSO	ω	[0.9, 0.4]
	c_1, c_2	2
PSOEM-FSA	ξ_t	0.5
	ξ_{t-1}	0.5
PSO-FSA	*Visual*	[*MaxD, 0.01MaxD*]
	Step	[*MaxD/5*, 0]
FSA	*Try_number*	5
	δ	0.75

PSO, particle swarm optimization; FSA, fish-swarm algorithm; PSOEM-FSA particle swarm optimization with extended memory of FSA.

Optimization precision analysis. To describe the advantage of PSOEM-FSA vividly, the convergence graphs of four test functions are plotted in Figure 4, where the abscissa represents iterations, and the vertical axis represents the average optimization results, the value of which is respectively taken by log10.

Some insightful conclusions can be drawn from Table 3. Table 3 shows the comparison results in terms of the best, the average and the log values of the average of the results obtained by each algorithm under the budgeted FES over 50 independent runs.

From Figure 4, it is clear that PSOEM-FSA consistently outperforms the other compared methods in the majority of the test functions. In addition, although PSOEM-FSA performs poorly on the single-peak function (Sphere), PSOEM-FSA significantly exceeds the FSA, PSO-FSA, and PSO on Quadric and Ackley functions. Furthermore, we can see from Table 3 that PSOEM-FSA promotes the performance on the most cases, especially in terms of the best on Sphere, Rosenbrock and Quadric functions.

It can be observed from Figure 4 and Table 3 that PSOEM-FSA exhibits faster convergence speed and higher searching precision than other algorithms on all cases. This can be explained that PSOEM-FSA can make use of the historical information stored by the extended memory to optimize the fish behaviour and control the fish to search for the promising food sources.

Volatility analysis of optimal results. To measure the merits of the algorithm performance, one of the criteria is to find out the optimal value with desired precision. After four algorithms independently operate 50 times, we obtain the standard deviations of 50 optimization results of four algorithms. Moreover, the standard deviations are used to reflect and compare the performance of four algorithms, and they are shown in Table 4 and Figure 6.

From Table 4 and Figure 6, it can be seen that the standard deviations of PSOEM-FSA are the smallest among the algorithms on the four test functions, indicating that the

Table 2. Benchmark test functions.

Function	Expression	Optimum value	Optimal range
Sphere	$f(x) = \sum_{i=1}^{n} x_i^2$	0	$(-100,100)^D$
Rosenbrock	$f(x) = \sum_{i=1}^{D-1} 100(x_{i+1} - x_i^2)^2 + (1 - x_i)^2$	0	$(-2.048,2.048)^D$
Quadric	$f(x) = \sum_{i=1}^{D} (\sum_{j=1}^{i} x_j)^2$	0	$(-100,100)^D$
Ackley	$f(x) = -20\exp(-0.2\sqrt{\frac{1}{D}\sum_{i=1}^{D} x_i^2}) - \exp(\frac{1}{D}\sum_{i=1}^{D}\cos(2\pi x_i))$	0	$(-32.768,32.768)^D$

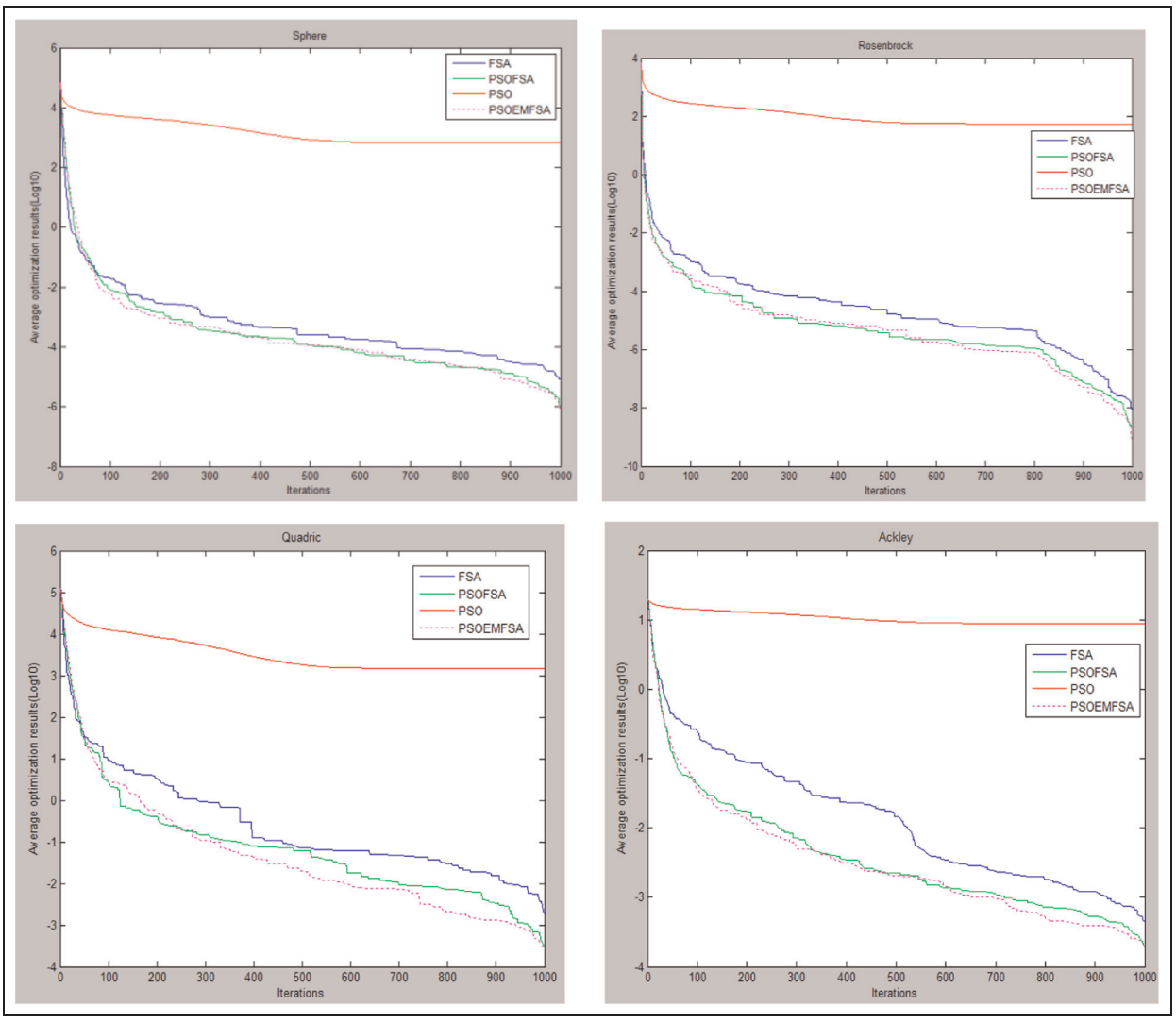

Figure 4. Convergence curves of four algorithms on four benchmark functions.

fluctuation of the optimization results of PSOEM-FSA is the smallest, and this algorithm can guarantee higher accuracy.

Algorithm time complexity analysis. The algorithm complexity is another standard to measure the merits of algorithm. Here, we compare the time complexity between PSOEM-FSA and the other algorithms. The convergence precision of the Quadric function is set to 1e-2, and the convergence precisions of other three functions are set to 1e-3. In addition, the other parameters of four algorithms are shown in Table 2. Four algorithms independently operate 50 times, and the

Table 3. Result comparison of four algorithms on four benchmark functions.

Function	Algorithm				
		PSO	FSA	PSO-FSA	PSOEM-FSA
Sphere	Best	3.751E-01	2.350E-09	3.753E-11	3.082E-13
	Average	2.185E + 02	2.384E-06	2.499E-07	6.185E-08
	Log10(average)	2.339	−5.623	−6.602	−7.207
Rosenbrock	Best	3.334E + 01	2.091E-11	4.024E-13	1.988E-14
	Average	1.383E + 02	6.877E-09	6.682E-09	6.55E-10
	Log10(average)	2.141	−8.16	−8.17	−9.18
Quadric	Best	3.545E + 02	3.883E-07	3.484E-07	1.163E-08
	Average	3.498E + 03	1.412E-02	3.110E-04	1.159E-04
	Log10(average)	3.544	−1.850	−3.507	−3.936
Ackley	Best	5.367 E + 00	1.786E-05	2.845E-07	1.684E-07
	Average	2.285 E + 00	8.720E-03	1.231E-04	1.018E-04
	Log10(average)	0.359	−2.059	−3.910	−3.992

PSO, particle swarm optimization; FSA, fish-swarm algorithm; PSOEM-FSA particle swarm optimization with extended memory of FSA.

Table 4. Standard deviations of optimization results of four algorithms.

Function	Algorithm			
	PSO	FSA	PSO-FSA	PSOEM-FSA
Sphere	1.525E + 03	8.726E-06	1.166E-06	1.113E-07
Rosenbrock	3.919E-01	2.784E-08	1.991E-09	1.866E-10
Quadric	6.538E + 03	2.604E-03	5.236E-04	2.625E-05
Ackley	5.799E + 00	3.492E-04	2.681E-04	1.106E-04

PSO, particle swarm optimization; FSA, fish-swarm algorithm; PSOEM-FSA particle swarm optimization with extended memory of FSA.

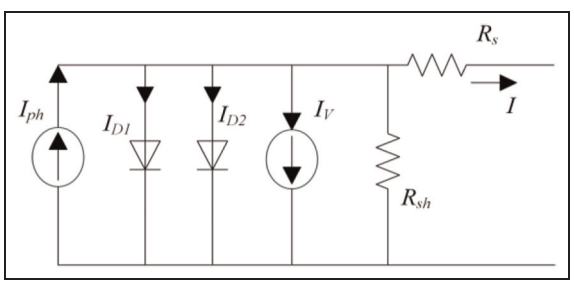

Figure 5. Equivalent circuit of photovoltaic cells under partial shading (PS) conditions.

iteration number and optimization time, which these algorithms achieved to the predetermined convergence precision, are shown in Table 5.

From Table 5, it is clear that the iteration number and optimization time that PSOEM-FSA requires is obviously less than the requirements of FSA and PSO-FSA. In particular, compared with FSA and PSO-FSA, PSOEM-FSA obviously performs the superiority on Rosenbrock and Quadric functions. Thus, the comparison result of the time complexity of FSA, PSO-FSA and PSOEM-FSA tested on the three functions again verify the effectiveness of PSOEM-FSA.

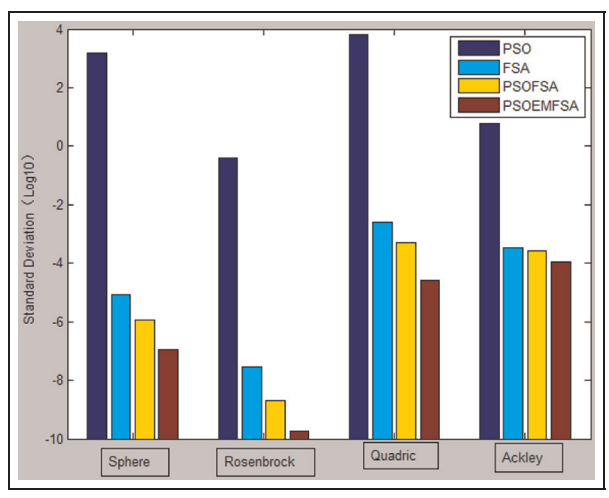

Figure 6. Standard deviations of optimization results of four algorithms.

Experiments of PV cells in series under PS conditions

Taking 10 PV cells in series as an example, when the whole cells are in at a temperature of 25°C and irradiance levels of 1000 W/m^2, the output power–voltage characteristic curve is shown in Figure 7. However, when they are at a temperature

Table 5. Result comparison of time complexity of FSA, PSO-FSA and PSOEM-FSA on three benchmark functions.

Function	FSA		PSO-FSA		PSOEM-FSA	
	Iterations	Time/s	Iterations	Time/s	Iterations	Time/s
Sphere	339.216	16.114	237.241	11.012	201.674	9.565
Rosenbrock	100.131	6.830	51.395	5.339	38.781	3.744
Quadric	894.788	63.347	664.685	52.672	601.330	35.213
Ackley	927.005	66.526	727.561	60.449	590.852	52.785

PSO, particle swarm optimization; FSA, fish-swarm algorithm; PSOEM-FSA particle swarm optimization with extended memory of FSA.

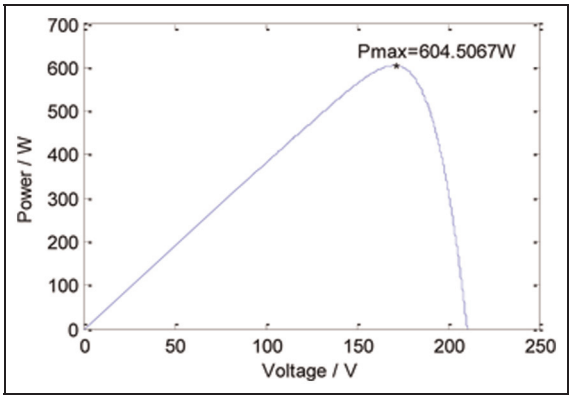

Figure 7. Output characteristics under illumination conditions.

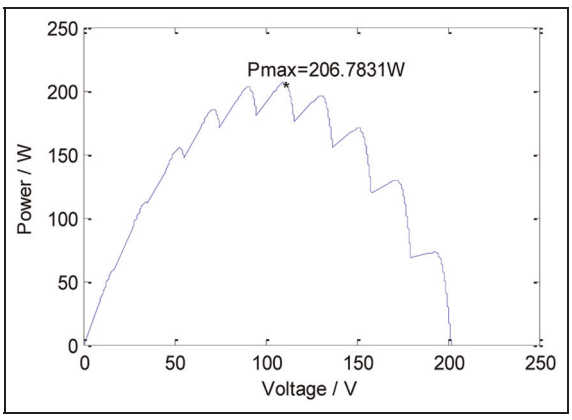

Figure 8. Output characteristics under partial shading (PS) conditions.

of 25°C and irradiance levels of 100, 200, 300, 400, 500, 600, 700, 800, 900 and 1000 W/m^2, the output power–voltage characteristic curve is shown in Figure 8. Figure 8 shows that the characteristic curve appears to be 10 peaks. Obviously, the existence of local minima will lead to failure of the conventional algorithm for MPPT.

The proposed algorithm for MPPT under PS conditions

In the simulation process, it is assumed that the temperature remains at 25°C. The short-circuit current of the arrays described by the Equation (12) at $T = 25$°C and Sun ≤ 1000 W/m^2 is no more than 4 A, so the optimal range of the algorithm is set to [0,5]. In addition, the fish scale is set to 5, the number of iterations is set to 10, the value of the MaxD should be set to 4 according to Equation (6), the values of ξ_t and ξ_{t-1} are separately set to 0.5 and 0.5 (Duan et al., 2011), and other parameters of PSOEM-FSA and PSOFSA are shown in Table 1.

The algorithms are independently run 10 times, and the results are shown in Table 6. In addition, the P&O method in engineering is also used in the environment to compare with PSOEM-FSA. The short-circuit current of the arrays described by the Equation (12) at $T = 25$°C and Sun ≤ 1000 W/m^2 was no more than 4 A, so the working point current of disturbance observation randomly was initialized within the range of [1.5,2.5] to simulate the working point of PV system before the PS conditions appeared. The perturbation step length of the P&O method is set to 0.05, and the number of iterations is set to 50.

Some insightful conclusions can be drawn from Table 6. PSOEM-FSA performs significantly better than the other algorithms compared on the most cases. In particular, PSOEM-FSA can catch the MPP with higher precision and output more power than PSO-FSA and P&O methods. To sum up, PSOEM-FSA obviously improves the reliability and effectiveness of MPPT for the PV system under PS conditions.

Simulation analysis on the experimental platform

The above described control algorithm was applied to control the PV system. The simulation model of PV array is made of two PV cells, which are connected in series. The block diagram of MPPT system (Veerachary et al., 2002) is shown in Figure 9.

In order to compare the simulations more easily, a boost control circuit adopts the resistance as the load. The MPPT controller respectively adopts the PSOEM-FSA method, PSO-FSA method and the traditional point-by-point comparison method to change the duty ratio D to generate the control signal through the pulse generator to drive the boost control circuit. In addition, the two PV cells of the PV array are at a temperature of 25°C and the irradiance levels are 1000 and 600 W/m^2, respectively (in short, $G_1 = 1000$ and $G_2 = 600$). The parameters in the simulation are as follows: boost inductor $L = 6.6$ mH, filter capacitor $C_1 = 82$ μF, capacitor of DC bus $C_2 = 47$ μF and load $R = 40$ Ω.

Table 6. Maximum power point tracking (MPPT) result comparison of PSOEM-FSA, PSO-FSA and P&O.

Running time		1	2	3	4	5	6	7	8	9	10
PSOEM-FSA	Pmax	206.2769	206.6168	206.1703	205.2306	206.6296	206.1092	206.5491	206.0533	206.2959	206.5236
	Error	0.2448%	0.0804%	0.2963%	0.7508%	0.0742%	0.3259%	0.1132%	0.3529%	0.2356%	0.1255%
PSO-FSA	Pmax	203.4938	204.0306	204.0560	206.4671	205.6646	204.1023	205.3348	205.7100	204.4318	206.1601
	Error	1.5907%	1.3311%	1.3188%	0.1528%	0.5409%	1.2964%	0.7004%	0.5189%	1.1371%	0.3013%
P&O	Pmax	183.6564	201.3178	199.9402	193.8293	202.9626	172.0312	180.8131	195.5924	200.6064	195.6503
	Error	11.1840%	2.6430%	3.3092%	6.2644%	1.8476%	16.8060%	12.5591%	5.4118%	2.9870%	5.3838%

PSO, particle swarm optimization; FSA, fish-swarm algorithm; PSOEM-FSA particle swarm optimization with extended memory of FSA; P&O, perturb and observe.

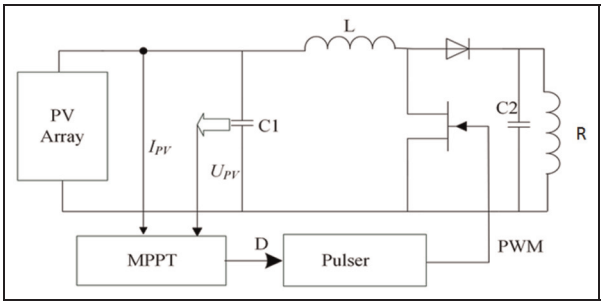

Figure 9. Photovoltaic (PV) system with maximum power point tracking (MPPT). Schematic of the experimental modelling and control scheme.

Results and discussions. In order to test the effectiveness of the PSOEM-FSA method, this method is compared with the PSO-FSA method and the traditional point-by-point comparison method in the different shading situation. Results and comparative analysis are as follows.

System voltages at different shading conditions by adopting the three methods are plotted in Figures 10–12 respectively, where the abscissa represents the times, and the vertical axis represents the voltage values. In Figures 10–12, Vout represents the total voltage value of the two PV cells, V1 represents the voltage value when the irradiance of the PV cell (G_1) is 1000 W/m^2 and V2 represents the voltage value when the irradiance of the other cell (G_2) is 600 W/m^2. What is more, Tables 7–9 show the output voltage values of the three methods when G_1 remains at 1000 W/m^2 and G_2 changes from 1000 to 100 W/m^2.

It can be observed from Figures 10 and 11, and Tables 7 and 8, that PSOEM-FSA consistently outperforms the PSO-FSA methods on the stability of the output voltages in most cases. From Figures 10–12 and Tables 7–9, it is also clear that the voltage values tested on the traditional point-by-point comparison method are more stable, but the voltage average values tested on PSOEM-FSA method are higher than the values tested on the other two methods.

Furthermore, Figure 13 shows the output power curves of the three methods. From Figure 13, it can be seen that the PSOEM-FSA method consistently outperforms the PSO-FSA method and the traditional point-by-point comparison method in the first stage ($t = 0$ to $t = 0.02$). In the second stage ($t = 0.02$ to $t = 0.06$), although the traditional point-by-point comparison method outperforms the PSOEM-FSA method and the PSO-FSA method on the stability of the output power, the PSOEM-FSA method obviously improves the output power of the PV array when compared with the other two methods.

Table 10 shows the output power values of the three methods when G_1 remains at 1000 W/m^2 and G_2 changes from 1000 to 100 W/m^2. Some insightful conclusions can be drawn from Table 10, showing that the PSOEM-FSA method consistently outperforms the PSO-FSA method and the traditional point-by-point comparison method on the stability of the output power when the PV system is under various PS conditions.

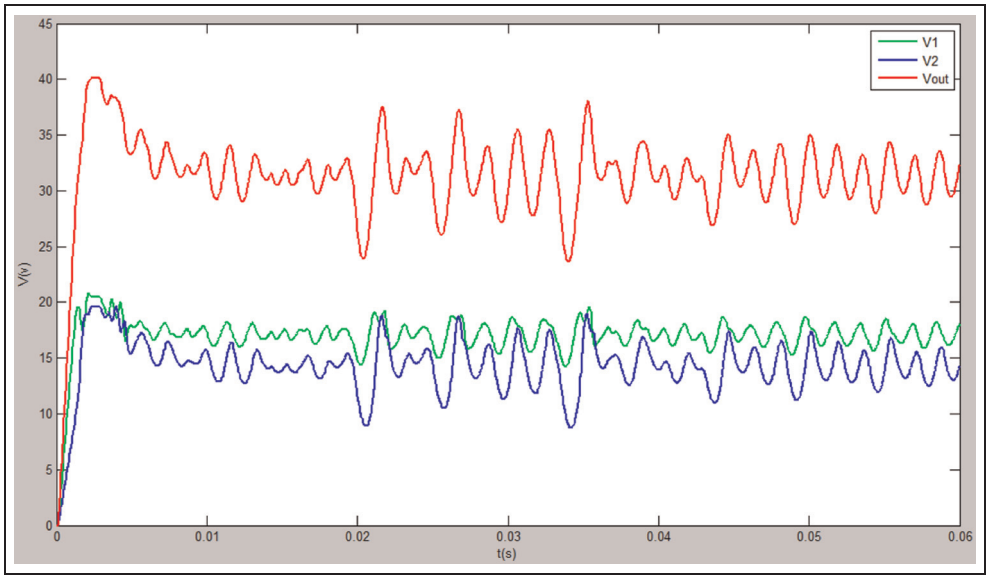

Figure 10. System voltages tested on the particle swarm optimization with extended memory of fish-swarm algorithm (PSOEM-FSA) method at different shading conditions (G_1=1000 and G_2=600).

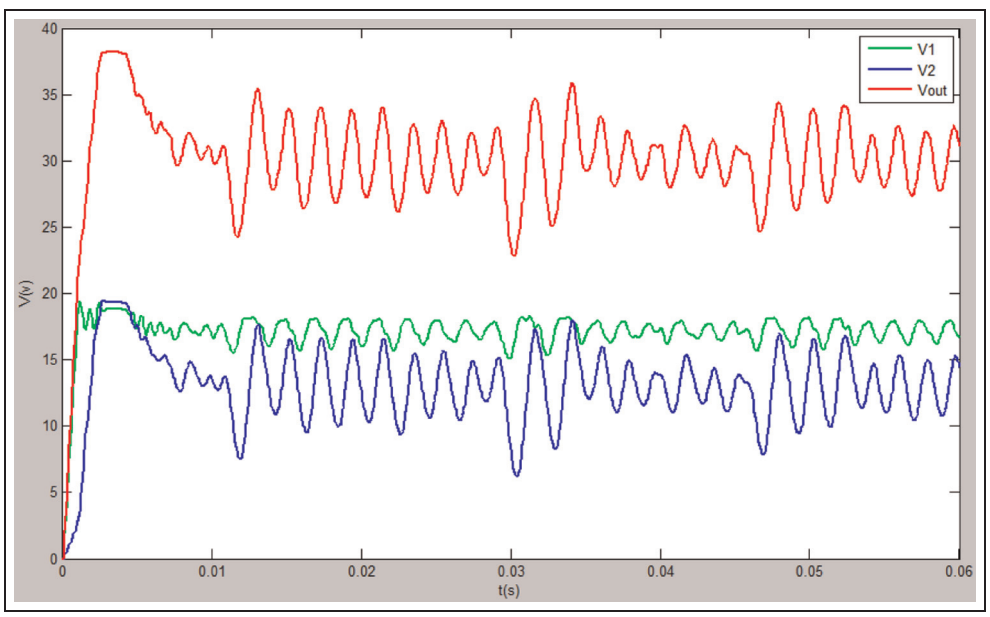

Figure 11. System voltages tested on the particle swarm optimization of fish-swarm algorithm (PSO-FSA) method at different shading conditions (G_1=1000 and G_2=600).

Table 7. Output voltages of the particle swarm optimization with extended memory of fish-swarm algorithm (PSOEM-FSA) method.

G_1 (kW/m^2)	G_2 (kW/m^2)	V1 (V)	V2 (V)	Vout (V)
1000	1000	18.21	18.13	36.34
1000	900	18.24	18.02	36.26
1000	800	18.19	17.98	36.17
1000	700	18.32	17.94	36.26
1000	600	18.26	17.83	36.09
1000	500	18.25	17.65	35.90
1000	400	18.18	17.60	35.78
1000	300	18.20	17.58	35.78
1000	200	18.23	16.78	35.01
1000	100	18.13	15.31	33.44

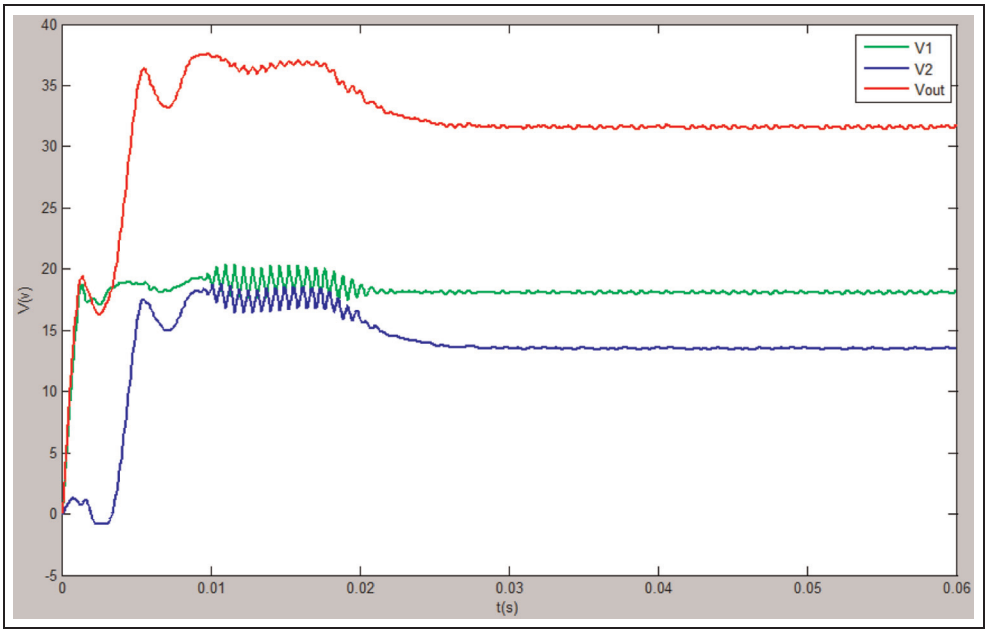

Figure 12. System voltages tested on the traditional point-by-point comparison method at different shading conditions (G_1=1000 and G_2=600).

Table 8. Output voltages of the particle swarm optimization–fish-swarm algorithm (PSO-FSA) method.

G_1 (kW/m^2)	G_2 (kW/m^2)	V1 (V)	V2 (V)	Vout (V)
1000	1000	17.40	17.18	34.58
1000	900	17.11	16.82	33.93
1000	800	17.39	16.20	33.59
1000	700	17.76	15.91	33.67
1000	600	17.82	16.13	33.95
1000	500	17.55	15.48	33.03
1000	400	17.92	14.26	32.18
1000	300	18.12	−1.11	17.01
1000	200	17.71	−1.24	16.47
1000	100	18.02	−1.37	16.65

Table 9. Output voltages of the traditional point-by-point comparison method.

G_1 (kW/m^2)	G_2 (kW/m^2)	V1 (V)	V2 (V)	Vout (V)
1000	1000	18.18	17.68	35.86
1000	900	17.94	17.25	35.19
1000	800	17.30	16.01	33.31
1000	700	16.55	15.33	31.88
1000	600	17.42	15.89	33.31
1000	500	17.98	15.38	33.36
1000	400	18.01	16.01	34.02
1000	300	16.78	−2.02	14.76
1000	200	17.68	−2.15	15.53
1000	100	18.07	−2.33	15.74

Conclusions

In this paper, a new intelligent algorithm called PSOEM-FSA is proposed and applied to MPPT of the PV system under PS conditions. Finally, the different tracking simulation tests have been performed and the three control methods were applied to control the PV system on the experimental platform to verify the effectiveness of the PSOEM-FSA method.

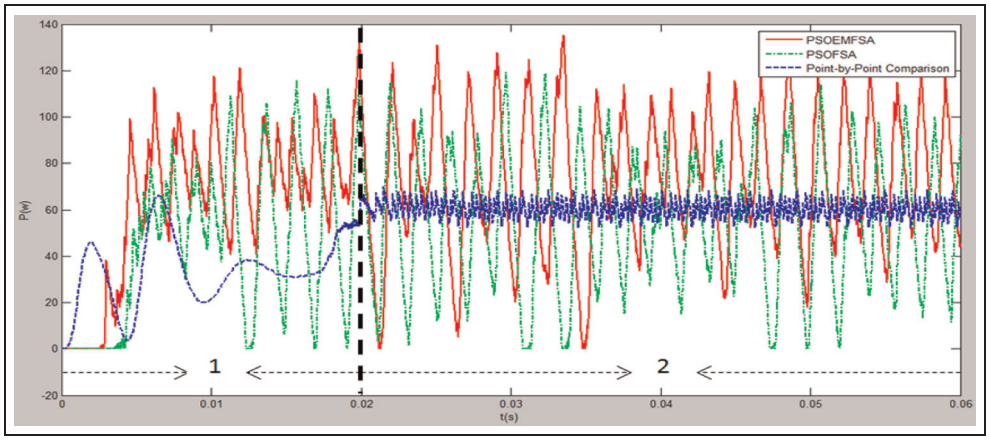

Figure 13. Output power curves of the three methods.

Table 10. Comparison of output power of the three methods.

G_1 (kW/m^2)	G_2 (kW/m^2)	PSOEM-FSA (W)	PSO-FSA (W)	Point-by-point comparison (W)
1000	1000	90.15	91.54	92.51
1000	900	89.64	88.61	89.67
1000	800	86.33	80.27	79.20
1000	700	81.57	72.18	68.13
1000	600	75.46	61.24	60.88
1000	500	69.35	50.71	51.14
1000	400	59.79	41.60	39.26
1000	300	50.11	36.15	32.73
1000	200	43.91	32.01	30.67
1000	100	37.14	29.46	28.06

PSO, particle swarm optimization; FSA, fish-swarm algorithm; PSOEM-FSA particle swarm optimization with extended memory of FSA.

Experimental results show that the PSOEM-FSA method can easily avoid the constraint of multiple local extreme value points, and catch the MPP of the current environment with high precision. Compared with the other methods, the proposed method obviously improves the reliability and effectiveness of MPPT for the PV system under PS conditions.

There are mainly two ways in which the performance of the MPPT algorithm could be further improved in future work. Firstly, the extended memory factor (ξ_{t-1}) can be set according to the non-uniform degree of PS conditions. In addition, the artificial fish of PSOEM-FSA are able to adjust their own visual and step length automatically to improve the reliability and effectiveness of MPPT further under PS conditions.

Acknowledgements

The authors would like to thank all the reviewers for very helpful comments and suggestions. This work has been supported by National Natural Science Foundation of China, No. 51377187.

Conflict of interests

The authors declare that there is no conflict of interests regarding the publication of this article.

Funding

This research was funded by National Natural Science Foundation of China 10.13039/501100001809 No. 51377187.

References

Agorreta JL, Borrega M, Lopez J, et al. (2011) Modeling and control of N-paralleled grid-connected inverters with LCL filter coupled due to grid impedance in PV plants. *IEEE Transactions on Power Electronics* 26(3): 770–785.

Alajmi BN, Ahmed KH, Finney SJ, et al. (2011) Fuzzy-logic-control approach of a modified hill-climbing method for maximum power in micro grid standalone PV systems. *IEEE Transactions on Power Electronics* 26(4): 1022–1030.

Banks A, Vincent J and Anyakoha C (2007) A review of particle swarm optimization. Part I: background and development. *Natural Computing* 6(4): 467–484.

Carannante G, Fraddanno C, Pagano M, et al. (2009) Experimental performance of MPPT algorithm for photovoltaic sources subject to inhomogeneous insolation. *IEEE Transactions on Industrial Electronics* 56(11): 4374–4380.

Duan QC, Huang DW, Lei L, et al. (2011) Simulation analysis of particle swarm optimization algorithm with extended memory. *Control and Decision* 26(7): 1087–1100.

Duan QC, Tang RL, Xu HY, et al. (2013) Simulation analysis of the fish swarm algorithm optimized by PSO. *Control and Decision* 28(9): 1436–1440.

Femia N, Petrone G, Spagnuolo G, et al. (2005) Optimization of perturb and observe maximum power point tracking method. *IEEE Transactions on Power Electronics* 20(4): 963–973.

Femia N, Petrone G, Spagnuolo G, et al. (2011) A technique for improving P&O MPPT performance of double-stage grid-connected photovoltaic systems. *IEEE Transactions on Industrial Electronics* 58(11): 76–84.

Figueres E, Garcera G, Sandia J, et al. (2009) Sensitivity study of the dynamics of three-phase photovoltaic inverters with an LCL grid filter. *IEEE Transactions on Industrial Electronics* 56(3): 706–717.

Ishaque K, Salam Z, Amjad M, et al. (2012) An improved particle swarm optimization (PSO)–based MPPT for PV with reduced steady-state oscillation. *IEEE Transactions on Power Electronics* 27(8): 3627–3638.

Kadri R, Gaubert JP and Champenois G (2011) An improved maximum power point tracking for photovoltaic grid-connected inverter based on voltage-oriented control. *IEEE Transactions on Industrial Electronics* 58(1): 66–75.

Lei P, Li YY and Seem JE (2011) Sequential ESC-based global MPPT control for photovoltaic array with variable shading. *IEEE Transactions on Sustainable Energy* 2(3): 348–358.

Liu BY, Duan SX and Cai T (2011) Photovoltaic DC-building-module based BIPV system – concept and design considerations. *IEEE Transactions on Power Electronics* 26(5): 1418–1429.

Li XL, Shao ZJ and Qian JX (2002) An optimizing method based on autonomous animats: Fish-swarm algorithm. *Systems Engineering-Theory & Practice* 22(11): 32–38.

Mei Q, Shan M, Liu L, et al. (2011) A novel improved variable step-size incremental-resistance MPPT method for PV systems. *IEEE Transactions on Industrial Electronics* 58(6): 2427–2434.

Messai A, Mellit A, Guessoum A, et al. (2011) Maximum power point tracking using a GA optimized fuzzy logic controller and its FPGA implementation. *Solar Energy* 85(2): 265–277.

Nopporn P, Suttichai P and Yosanai S (2005) Maximum power point tracking using adaptive fuzzy logic control for grid-connected photovoltaic system. *Renewable Energy* 30(11):1771–1788.

Patel H and Agarwal V (2008) Maximum power point tracking scheme for PV systems operating under partially shaded conditions. *IEEE Transactions on Industrial Electronics* 55(4): 1689–1698.

Safari A and Mekhilef S (2011) Simulation and hardware implementation of incremental conductance MPPT with direct control method using cuk converter. *IEEE Transactions on Industrial Electronics* 58(4): 1154–1161.

Serban E and Serban H (2010) A control strategy for a distributed power generation microgrid application with voltage- and current-controlled source converter. *IEEE Transactions on Power Electronics* 25(12): 2981–2992.

Syafaruddin R, Karatepe E and Hiyama T (2009) Artificial neural network-polar coordinated fuzzy controller based maximum power point tracking control under partially shaded conditions. *IET Renewable Power Generation* 3(2): 239–253.

Veerachary M, Senjyu T and Uezato K (2002) Feedforward maximum power point of PV systems using fuzzy controller. *IEEE Transactions on Aerospace and Electronic Systems* 38(3): 969-981.

Wang YJ and Hsu PC (2010) Analytical modelling of PS and different orientation of photovoltaic modules. *IET Renewable Power Generation* 4(3): 272–282.

Yang B, Li WH, Zhao Y, et al. (2010) Design and analysis of a grid connected photovoltaic power system. *IEEE Transactions on Power Electronics* 25(4): 992–1000.

Young-Hyok J, Doo-Yong J, Chung-Yuen W, et al. (2011) A real maximum power point tracking method for mismatching compensation in PV array under partially shaded conditions. *IEEE Transactions on Power Electronics* 26(4): 1001–1009.

Zhang L, Sun K, Xing Y, et al. (2011) A modular grid connected photovoltaic generation system based on DC bus. *IEEE Transactions on Power Electronics* 26(2): 523–531.

Zhan ZH, Zhang J, Li Y, et al. (2009) Adaptive particle swarm optimization. *IEEE Transaction on System, Man and Cybernetics, Part B: Cybernetics* 39(6): 1362–1381.